Published in final edited form as:
Langmuir. 2006 May 9; 22(10): 4699–4709. doi:10.1021/la053242r.

Exploring the Interaction of Ruthenium(II) Polypyridyl Complexes with DNA Using Single-Molecule Techniques†

Aleksandra Mihailovic‡, **Ioana Vladescu**§, **Micah McCauley**§, **Elaine Ly**⊥, **Mark C. Williams**§, **Eileen M. Spain**⊥, and **Megan E. Nuñez***,‡

‡ *Department of Chemistry, Mount Holyoke College, South Hadley, Massachusetts 10075*

§ *Department of Physics, Northeastern University, Boston, Massachusetts 02115*

⊥ *Department of Chemistry, Occidental College, Los Angeles, California 10021*

Abstract

Here we explore DNA binding by a family of ruthenium(II) polypyridyl complexes using an atomic force microscope (AFM) and optical tweezers. We demonstrate using AFM that $Ru(bpy)_2dppz^{2+}$ intercalates into DNA ($K_b = 1.5 \times 10^5\ M^{-1}$), as does its close relative $Ru(bpy)_2dppx^{2+}$ ($K_b = 1.5 \times 10^5\ M^{-1}$). However, intercalation by $Ru(phen)_3^{2+}$ and other Ru(II) complexes with K_b's lower than $Ru(bpy)_2dppz^{2+}$ are difficult to determine using AFM because of competing aggregation and surface-binding phenomena. At the high Ru(II) concentrations required to evaluate intercalation, most of the DNA strands acquire a twisted, curled conformation that is impossible to measure accurately. The condensation of DNA on mica in the presence of polycations is well known, but it clearly precludes the accurate assessment by AFM of DNA intercalation by most Ru(II) complexes, though not by ethidium bromide and other monovalent intercalators. When stretching individual DNA molecules using optical tweezers the same limitation on high metal concentration does not exist. Using optical tweezers we show that $Ru(phen)_2dppz^{2+}$ intercalates avidly ($K_b = 3.2 \times 10^6\ M^{-1}$) while $Ru(bpy)_3^{2+}$ does not intercalate, even at micromolar ruthenium concentrations. $Ru(phen)_3^{2+}$ is shown to intercalate weakly, i.e. at micromolar concentrations ($K_b = 8.8 \times 10^3\ M^{-1}$). The distinct differences in DNA stretching behavior between $Ru(phen)_3^{2+}$ and $Ru(bpy)_3^{2+}$ clearly illustrate that intercalation can be distinguished from groove binding by pulling the DNA with optical tweezers. Our results demonstrate both the benefits and challenges of two single-molecule methods in exploring DNA binding, and help to elucidate the mode of binding of $Ru(phen)_3^{2+}$.

Introduction

The binding to DNA of ruthenium(II) polypyridyl complexes has been studied for about 20 years. [1-10] This group of octahedral organometallic complexes has been used to explore aspects of DNA structure, details of how small molecules bind to DNA, and techniques that inform us about DNA binding. The basic motif, a Ru(II) center surrounded by three heterocyclic, aromatic bidentate ligands, has provided a convenient three-dimensional scaffold

†This work was supported by the Camille and Henry Dreyfus Foundation (M.E.N.), the Clare Boothe Luce Foundation (M.E.N.), the National Science Foundation (#CHE9703345 to E.M.S., #CHE0320542 to M.E.N., #MCB0238190 to M.C.W.), the NIH (GM-072462 to M.C.W.), the ACS Petroleum Research Fund (M.C.W), and the Research Corporation (M.C.W).

* To whom correspondence should be addressed: Department of Chemistry, Mount Holyoke College, South Hadley, MA 10075. Telephone: (413) 538−2449; Fax: (413) 538−2327; E-mail: menunez@mtholyoke.edu.

Supporting Information Supporting information is available free of charge via the Internet at http://pubs.acs.org. DNA length histograms for $Ru(phen)_3^{2+}$, $Ru(bpy)_3^{2+}$, $Ru(bpy)_2dppx^{2+}$, and $Ru(bpy)_2dpq^{2+}$ determined by atomic force microscopy are available as supplementary materials Figs. 1supp-4supp.

for building a family of complexes with different shapes, sizes, functional groups, and properties. In general, these complexes bind noncovalently to DNA by a combination of electrostatic and van der Waals effects, but their binding constants, exchange rates, and means of interaction with the DNA vary. Most have useful and interesting photophysical and redox properties that can inform us about DNA. They absorb visible light allowing a metal-to-ligand charge transfer (MLCT), and binding to DNA can perturb this transition. Most interestingly, the dipyridophenazine (dppz) complexes of ruthenium are “light switches” that luminesce when they bind to DNA.[11] Many of these complexes also can oxidize guanine bases on DNA using either a “flash-quench” method or via singlet oxygen sensitization.[12,13]

In this paper we will discuss several of these complexes, shown in figure 1: $Ru(bpy)_2dppz^{2+}$, $Ru(phen)_3^{2+}$, $Ru(bpy)_3^{2+}$, $Ru(bpy)_2dppx^{2+}$, $Ru(phen)_2dppz^{2+}$, and $Ru(bpy)_2dpq^{2+}$ (bpy=bipyridine; phen=1,10-phenanthroline; dppz= dipyrido[3,2-a:2’,3’]phenazine; dppx=7,8-dimethyldipyridophenazine; dpq=dipyridoquinoxaline). All share the same basic shape and charge, but have a unique complement of ligands that effects their interaction with DNA. The $Ru(bpy)_2dppz^{2+}$ and $Ru(phen)_2dppz^{2+}$complexes bind strongly to DNA by intercalating the large aromatic dppz ligand in between the base pairs.[8,14] $Ru(bpy)_3^{2+}$, on the other hand, has only small bipyridine ligands and thus binds DNA weakly and electrostatically.[3] Of intermediate size is the trisphenanthroline complex $Ru(phen)_3^{2+}$ whose mode of binding is more complex and controversial. It has been reported to bind intercalatively, electrostatically (i.e. non-intercalatively in one of the DNA grooves), and semi- or quasi-intercalatively by different groups using different experimental methods.[2, 4-7, 15-17] The other two complexes with dppz-based ligands, $Ru(bpy)_2dppx^{2+}$ and $Ru(bpy)_2dpq^{2+}$, have been less well characterized but appear to bind by intercalation.[10,13,18,19] In this work the binding of these complexes to DNA is explored using AFM and optical tweezers. Though atomic force microscopes and optical tweezers both are “single molecule” instruments, they have unique operational principles and measure different properties of the DNA. As a result, each has the potential to provide unique information about the binding of ruthenium(II) polypyridyl complexes.

When an intercalator binds, DNA opens up and unwinds to accommodate it between the base pairs.[20] In the process, the DNA helix gets longer. Thus, if we measure the length of a piece of DNA, add molecule of interest, and observe that the DNA gets longer, we can conclude that this molecule is an intercalator. The amount of increase in DNA length is directly related to the number of molecules that bind to a piece of DNA and thus can be used to determine the binding constant. Atomic force microscopy (AFM) is a scanning probe technique in which a small, sharp tip is scanned across a surface. Small variations in the height of the surface cause deflections of the probe, and these deflections are then translated into an image. This process can resolve objects in the nanometer to micron regime, allowing us to image and measure the dimensions of individual macromolecules supported on a solid surface. By establishing an increase in the length of individual DNA strands, atomic force microscopy has been used successfully to demonstrate the intercalation of several organic molecules, including the classic intercalator ethidium.[21-25]

When an intercalator binds, the additional hydrophobic stacking of the molecule with the base pairs not only lengthens the DNA but also stabilizes the DNA double helix. As a result, it is more difficult to pull the two strands of the helix apart, and the melting temperature of the DNA increases. Thus, techniques that measure the melting of the two DNA strands can also provide important information about binding of molecules to DNA. Such a technique is DNA pulling using optical tweezers. Optical tweezers have been used previously to stretch individual pieces of double-stranded DNA, measure the contour length of the DNA and forces required to pull the two DNA strands apart, and thereby elucidate DNA binding and stabilization by

various proteins and ions.[26-29] The method of DNA stretching has also been used successfully to examine binding by simple intercalators and groove binders.[30-35]

In this work we have two complementary goals for using AFM and optical tweezers to explore the binding of several ruthenium(II) complexes. First, DNA length measurements with AFM and DNA stretching with optical tweezers were explored to determine what new information these methods might reveal about the binding of Ru(II) polypyridyl molecules in particular. Because the binding of these molecules is complex and various bulk methods have provided complicated complementary or even contradictory information, any new information about their binding behavior may improve our understanding of this system. More generally, both methods have been used previously to examine DNA binding by small molecules with a single binding mode. It is our second, broader goal to determine whether these techniques can be used productively to study molecules (like many of the Ru(II) polypyridyl complexes) that have multiple binding modes and complicated interactions with DNA.

Experimental Procedures

Ruthenium complexes

Ligands and octahedral ruthenium complexes for the AFM experiments were prepared and characterized using published techniques.[10,13,14,36] $Ru(phen)_3^{2+}$ and $Ru(bpy)_3^{2+}$ for the optical tweezers experiments were obtained commercially (Sigma). Racemic mixtures were used in all cases.

The complexes were quantitated spectrophotometrically using the following molar absorptivity constants[13]: $Ru(bpy)_2dppz^{2+}$: ε_{440}=21,400 $M^{-1}cm^{-1}$. $Ru(phen)_3^{2+}$: ε_{447}=19,000 $M^{-1}cm^{-1}$. $Ru(bpy)_3^{2+}$: ε_{452}: 14,000 $M^{-1}cm^{-1}$. $Ru(bpy)_2dppx^{2+}$: ε_{450}=21,000 $M^{-1}cm^{-1}$. $Ru(bpy)_2dpq^{2+}$: ε_{450}=14,200 $M^{-1}cm^{-1}$. $Ru(phen)_2dppz^{2+}$: ε_{440}=21,000 $M^{-1}cm^{-1}$.

AFM Experiments

Purified plasmid DNA pBR322 was obtained commercially from New England Biolabs. The DNA was cut with PvuII to generate blunt ends and was repurified by extraction with phenol and chloroform and ethanol precipitation. The DNA was resuspended in 1X TE (10 mM Tris pH 7.5, 1 mM EDTA) and was quantitated by ultraviolet absorbance prior to use.

High-quality mica sheets (Asheville-Shoonmaker Mica) were cut with scissors into squares (~1cm × 1 cm) and attached with superglue to 15 mm round stainless-steel sample discs (Ted Pella). Before each use the mica was freshly cleaved by pulling off the top sheets with tape and then was covered with 10 μL of autoclaved AFM buffer (10 mM Tris pH 7.5, 1 mM EDTA, 5 mM MgCl). The surface is precoated with Mg^{2+} in order to prevent Ru(II) binding to the surface, while allowing negatively-charged DNA to bind. After 5 minutes the buffer was rinsed thoroughly with ~5 mL of distilled water and the mica was briefly dried under a stream of N_2(g).

To deposit the DNA on the mica surface, the stock solution of DNA was freshly diluted to 750 nM base pairs in AFM buffer and gently warmed to 37°C to reduce clumping of the DNA. After cooling the DNA to room temperature, the ruthenium complex was added, and 5 μL of this mix was placed on the buffer-coated mica. Five minutes later the DNA and buffer solution was rinsed with ~5 mL of distilled water, and the mica was briefly dried under a stream of N_2(g) before imaging.

AFM measurements were performed on a Multimode SPM with a Nanoscope IV controller or with a Dimension 5100 AFM with a Nanoscope III controller (both from Veeco/Digital Instruments). Samples were imaged in tapping mode in air using oxide-sharpened silicon tips

with cantilever resonance frequencies around 300 kHz (Veeco). Only one modification to the images was performed as provided by the image software: the vertical offset between scan lines was removed, termed flattening. For a given image, this was accomplished by subtraction of the average vertical value of the scan line from each point in the scan line. The DNA lengths were determined manually by tracing individual molecules and summing the length of the traces in the offline programs of the Nanoscope software.

Fitting of AFM Data

Measured DNA lengths were plotted as histograms. Representative lengths were determined in three ways: means, medians, and fitting a Gaussian to the histogram. All three methods gave similar results, so lengths were determined by fitting a Gaussian to the histogram for the purposes of this analysis. The error in the lengths represents the combination of the uncertainty in fitting the Gaussian for the DNA alone and the DNA with ruthenium added in quadrature.

Next the average lengths were fitted to a simple equilibrium binding expression. Briefly, for the binding equilibrium

$$\mathrm{Ru + DNA} \qquad (\mathrm{Ru{-}DNA\ \ complex}) \tag{1}$$

the binding expression is

$$K_b = [\mathrm{Ru{-}DNA}] / [\mathrm{Ru}]\,[\mathrm{DNA}] \tag{2}$$

The measured lengths of the DNA at each Ru concentration are used to calculate [Ru-DNA] (assuming 0.34 nm lengthening per intercalation and 172 pM DNA strands):

$$[\mathrm{Ru{-}DNA}] = \left(\frac{\text{measured length} - \text{unintercalated length}}{0.34\ \ \mathrm{nm}}\right)^{*} 1.72 \times 10^{-10}\ \ \mathrm{M} \tag{3}$$

[Ru] is simply the initial Ru concentration minus the bound:

$$[\mathrm{Ru}] = [\mathrm{Ru}]_0 - [\mathrm{Ru{-}DNA}] \tag{4}$$

The [DNA] is the initial DNA concentration minus the bound. But what is the initial DNA concentration? This factor must take into account not just all of the base pairs (750 nm) but *also* the neighbor exclusion number (n):

$$[\mathrm{DNA}] = (750\ \ \mathrm{nM}\ \ /\ \ \mathrm{n}) \ - \ [\mathrm{Ru{-}DNA}] \tag{5}$$

Thus there are two unknowns, K_b and n. To determine both, the equations 3, 4, and 5 were substituted back into equation 2; the modified equation was then rearranged algebraically, and the data were fitted in Gnuplot to the resulting quadratic equation to solve for K_b and n using a Marquardt-Levenberg downhill fitting algorithm.[37]

DNA Stretching Experiments

Purified phage lambda DNA (~48,000 bp) was obtained commercially from New England Biolabs. The DNA was labeled with biotin at its 3' ends and was repurified by extraction with phenol and chloroform and ethanol precipitation. The DNA was resuspended in 10 mM Hepes pH 7.5 and 100 mM Na^+ (95 mM NaCl, 5 mM NaOH).

The optical tweezers experiments described here stretched the DNA between two beads (Fig 2a). As the force is increased and the double strand is melted, the structural parameters of the DNA double helix are revealed. Two beams (shown in red), each with approximately 150 mW of near-infrared light (JDS Uniphase), were focused to a diameter of approximately one micron using 60X water immersion objectives (Nikon). The focus of each counter-propagating beam overlapped in a flow cell (grey), forming the optical trap. A streptavidin-coated polystyrene

bead with a diameter of 5 μm (Bangs Labs) was held in the trap, while another was attached to a micropipette tip (World Precision Instruments). The buffer solution containing biotin-labeled phage lambda DNA (shown in black) was introduced into the cell allowing DNA attachment between the beads. The micropipette tip, mounted on a piezoelectric stage (Melles Griot), was moved, causing the DNA to stretch between the two beads. As the force on the DNA increased, the bead in the optical trap was displaced, generating a beam deflection that was determined on the lateral effect detectors (Melles Griot) and recorded on custom-built software. This experimental setup has been previously described in more detail.[38]

DNA was stretched and relaxed repeatedly in the buffer described above at varying rates, though 250 nm per second was typical for the data presented here. A solution of varying concentrations of ruthenium(II) complex was added to the cell, and force curves were collected again. Though individual curves are shown here, multiple curves were collected at each concentration and with several different DNA molecules to determine the repeatability of the experiment and the error in the measurements.

Fitting of DNA Stretching Data

Typical force extension curves are shown in Figure 2b for a single molecule of phage lambda DNA in10 mM Hepes (pH 7.50), 50 mM Na^+. Solid and dashed lines show DNA extension and relaxation data, respectively. As the DNA is pulled, the length remains constant around 0.34 nm/base pair but the measured force increases until a force plateau is reached at ~ 65 pN. This plateau signals the cooperative melting transition to single stranded DNA. The further increase in force reveals the elasticity of the single stranded chain, which will finally break under forces of ~ 150 pN (not shown). Some hysteresis is observed as the strands re-anneal.

We recorded stretching – relaxation cycles for single DNA molecules in the absence and presence of different Ru(II) concentrations and measured the increase in contour length at constant force for each concentration. The ratio between the change in DNA extension (per base pair) due to the intercalation of drug, δb, and the saturation value of extension (per base pair), b_{max}, gave the fractional occupancy of ruthenium complex to dsDNA, Θ,

$$\Theta = \frac{\delta b}{b_{\max}} \tag{6}$$

This fractional occupancy was plotted as a function of drug concentration. The resulting binding curve was fitted with McGhee – von Hippel model [39,40] using the equation

$$\Theta = K_b \cdot n \cdot c \frac{(1-\Theta)^n}{(1-\Theta+\Theta/n)^{n-1}} \tag{7}$$

where K_b is drug binding constant, n is binding site size (in base pairs), and c is the ruthenium concentration. The data were fitted in Origin (Microcal, Northampton, MA) to equation 7 to solve for K_b ,n and b_{max} using a Marquardt-Levenberg fitting algorithm.

Results

AFM Measurements of DNA Lengths

In this work and many others, AFM has been used to image individual pieces of DNA on a mica surface.[41,42] These images of individual DNA molecules are particularly impressive considering that the double helix is less than 5 nm wide. Because of the resolution limit of the AFM, the DNA fragments look like squiggly lines; individual atoms cannot be resolved, nor generally can the grooves nor the helical twist, but the overall shape can be seen and the length can be measured with reasonable accuracy and precision (Fig. 3a).

The DNA that we chose to study is linearized plasmid pBR322, which is 4361 base pairs long. We expect this DNA to be 1.46 μm long based on a 0.34 nm rise per base pair. Interestingly, when several dozen molecules are imaged and their lengths are measured, we observe a *distribution* of lengths around 1.40 to 1.50 μm (Fig. 3b); thus, many of the molecules have lengths that are distinctly different than 1.46 μm. The distribution of lengths is not due entirely to measurement error; the general observation made by many biophysicists in recent years that individual molecules can be very different from one another and from the population average is one of the most interesting discoveries to come out of single molecule work. For our purposes the result of this observation is that in order to get reliable length measurements for DNA molecules, it was essential for us to measure many molecules under every experimental condition (generally between 100−300) and determine an average length for the population.

DNA Lengthening Measured by AFM for $Ru(bpy)_2dppz^{2+}$

We first studied the binding to DNA of $Ru(bpy)_2dppz^{2+}$ by AFM because the evidence is strong for intercalation of this complex. The DNA concentration, 750 nM base pairs, represented the optimal amount of DNA that was high enough to provide measurable numbers of DNA strands, but was just low enough to prevent DNA aggregation and condensation on the magnesium-coated mica surface. At moderate Ru:base pair ratios (below 1:1), no lengthening of the DNA was observed (data not shown). Based on previously published binding constants for intercalation by this complex and its closely-related cousin $Ru(phen)_2dppz^{2+}$ (K_b around 10^6 M^{-1} or lower in the presence of divalent cations[8,13]), the absence of intercalation at these concentrations is fully to be expected. It was necessary to increase the Ru concentration into the low micromolar regime in order to measure any lengthening due to $Ru(bpy)_2dppz^{2+}$ intercalation into DNA. These concentrations represent very high ruthenium to base pair ratios; though not ideal for measuring binding constants, these concentrations are required by the technique and have worked for other intercalators.[21-23]

Figure 4 shows representative images of DNA molecules and matching histograms of DNA lengths for a range of $Ru(bpy)_2dppz^{2+}$ concentrations. When the ruthenium concentration is increased from 750 nm to 1.2 μM, 3.0 μM, 6 μm, and 9 μM, the DNA begins to look very straight and line up on the surface. The mean length of the DNA also increases correspondingly, as seen from the length histograms (Fig. 4). This distinct increase in length confirms that $Ru(bpy)_2dppz^{2+}$ intercalates.

At 15 μM $Ru(bpy)_2dppz^{2+}$ and above, however, the surface is sometimes sticky, the DNA begins to curl up and condense, and some of the DNA molecules cannot be measured. At 25 μM and above the DNA is very condensed, and few molecules can be measured. Some appear anomalously short, probably due to curling in the Z-direction. At ruthenium concentrations above 38 μM we could not take data at all.

The measured length of the DNA plus $Ru(bpy)_2dppz^{2+}$ at each $Ru(bpy)_2dppz^{2+}$ concentration can be used to calculate directly the concentration of occupied sites (Eqn. 3). The binding titration curve, representing the relationship between metal complex concentration and occupied sites, is then plotted and fit as described in the methods section (Fig. 5). Between 750 nM and 12 μM $Ru(bpy)_2dppz^{2+}$, the occupancy increases as expected. The binding curve yields a binding constant of $(1.5 \pm 0.7) \times 10^5$ M^{-1} and a neighbor exclusion number n of 2.2 ± 0.4. However, it is clear (*particularly* from a logarithmic plot, as shown here) that the entire binding curve is not represented, specifically at saturating amounts of $Ru(bpy)_2dppz^{2+}$, which contributes to the uncertainties in both numbers.

DNA Lengthening Measured by AFM for $Ru(phen)_3^{2+}$ and other Ru(II) Complexes

Having established that this technique could be used to measure DNA lengthening and $Ru(bpy)_2dppz^{2+}$ complex intercalation within certain experimental limitations, we used the AFM to explore possible intercalation by $Ru(phen)_3^{2+}$ and other Ru(II) complexes including $Ru(bpy)_3^{2+}$, $Ru(bpy)_2dppx^{2+}$, and $Ru(bpy)_2dpq^{2+}$.

The concentration of occupied sites vs. the Ru(II) concentration was determined for $Ru(phen)_3^{2+}$, $Ru(bpy)_3^{2+}$, $Ru(bpy)_2dppx^{2+}$, and $Ru(bpy)_2dpq^{2+}$ as above. First, for each complex the lengths of several dozen to hundreds of molecules were measured at several different concentrations between the range of 1:1 and 50:1 Ru to base pairs. Since $Ru(bpy)_2dppz^{2+}$ did not intercalate below 1:1 Ru:base pairs and it is well-established to bind more strongly than the others, measurements were not done at lower Ru(II) concentrations; at higher Ru(II) concentrations than 37 μM, as with $Ru(bpy)_2dppz^{2+}$ the surface is greasy, the DNA curls up into loops and balls, and the lengths are difficult or impossible to determine (Fig. 6). Characteristic lengths were determined from histograms of individual measurements, and those lengths were used to compute the concentration of occupied sites. (Histograms for all four complexes at all concentrations are available as supplementary materials Figs. 1supp-4supp). Finally, the concentration of occupied sites was plotted as a function of ruthenium concentration for all five complexes (Fig. 7).

Within this range of concentrations, $Ru(bpy)_2dppx^{2+}$ shows measurable lengthening and intercalation just like its near relative $Ru(bpy)_2dppz^{2+}$. In fact, the points and fits nearly overlay, demonstrating that the two additional methyl groups on the dipyridophenazine ligand do not significantly perturb intercalation. The intercalation parameters for this complex are K_b of $(1.5 \pm 0.7) \times 10^5\ M^{-1}$ and n of 1.9 ± 0.4. Again the lengthening at saturating amounts of $Ru(bpy)_2dppx^{2+}$ cannot be determined, which contributes to the uncertainties of the fit.

The $Ru(phen)_3^{2+}$, $Ru(bpy)_3^{2+}$, and $Ru(bpy)_2dpq^{2+}$ complexes, however, show little or no DNA lengthening at all concentrations measured, demonstrating that they do not intercalate within the error of this experiment. It should be noted that the error bars for the measured lengths do not all overlap with the length of the DNA alone; most of the measured lengths are somewhat larger or smaller, but with no consistent pattern that can be fit to the binding expression (Eqn. 2) and reasonable values of n and K_b. This scatter tells us that the error bars determined from the Gaussian fits for a single data point do not take into account some additional source of point-to-point error that we were unable to identify conclusively. Nonetheless, this error corresponds to less than 10% of the overall length of the DNA, so lengthening by the $Ru(bpy)_2dppz^{2+}$ and $Ru(bpy)_2dppx^{2+}$ intercalators could be clearly identified.

A quick survey of the figure 7 makes it clear that this absence of lengthening does not necessarily mean that $Ru(phen)_3^{2+}$, $Ru(bpy)_3^{2+}$, and $Ru(bpy)_2dpq^{2+}$ do not intercalate. The absence of lengthening means only that intercalation cannot be measured within the proscribed concentration range, and thus cannot be measured by this method. The other complexes might behave consistently with these data and yet intercalate, but with K_b's below $10^4\ M^{-1}$. With a K_b below $10^4\ M^{-1}$, their binding curves would be shifted off the right side of the graph relative to the dppz and dppx complexes. Interestingly, the other three complexes behave relatively identically at this concentration range. The binding constants for intercalation estimated by AFM for all five ruthenium polypyridyl complexes are summarized in Table 1.

$Ru(phen)_2dppz^{2+}$ Intercalation Measured by DNA Stretching with Optical Tweezers

To further explore the interaction of Ru(II) polypyridyl complexes with DNA, we turned to DNA stretching measurements using optical tweezers. In the absence of any DNA binding molecule, the DNA undergoes a characteristic stretching transition from double-stranded to

single stranded DNA (Fig. 2b), but with increasing concentrations of $Ru(phen)_2dppz^{2+}$ in the nanomolar regime, the shape of the curves evolves in a distinctive way (Fig. 8a). First, the curves shift to the right, indicating that the contour length of the DNA molecule increases with the increase in ruthenium concentration. This increase saturates at a $Ru(phen)_2dppz^{2+}$ concentration of 750 nM. Simultaneously, the melting plateau becomes progressively shorter and occurs at higher forces, indicating that the dppz complex stabilizes the DNA duplex. This simultaneous increase in contour length and increase in the force required to melt the DNA occurs only for intercalating molecules, and thus these DNA pulling experiments clearly demonstrate that $Ru(phen)_2dppz^{2+}$ molecules intercalate into dsDNA.

Furthermore, these force data can be used to determine thermodynamic parameters for $Ru(phen)_2dppz^{2+}$ intercalation into DNA, specifically by examining the occupation of the DNA by intercalator at a range of concentrations but at a single low applied force. Figure 8b shows the intercalative binding curve for $Ru(phen)_2dppz^{2+}$ obtained at 10 pN force and its fit to the Mc Ghee-von Hippel model (Eqn. 7). The values obtained from this fit are $K_b = (3.2 \pm 0.1) \times 10^6\ M^{-1}$ and $n = 3 \pm 0.5$. The fit of the data to the Mc Ghee-von Hippel model is reasonable as seen from the overlap of the curve with almost all of the error bars and from the reduced χ^2 for the fit of 2.1. These values for K_b and n are also in good agreement with literature values from bulk measurements.[8] Similar values are obtained at forces of 5 pN and 20 pN.

The shape of the melting curves can provide other interesting information. The plateau exhibits a slope that increases with $Ru(phen)_2dppz^{2+}$ concentration and could suggest a reduction in cooperativity of the melting transition. In addition, there are some significant differences in stretching curve shape at low and high drug concentrations. This fact has important implications in measurement of binding constant and binding site size: the measured change in contour length, δb, and the calculated fractional occupancy, Θ, are different at forces greater than 30 pN, resulting in different values for K_b and n. We explain this unusual behavior of the stretching curves by the fact that high stretching forces (above 30 pN) destabilize the DNA base stacking and promote supplemental intercalation into the DNA molecule.[30]

Intercalation Confirmed for $Ru(phen)_3^{2+}$ and Ruled Out for $Ru(bpy)_3^{2+}$ Using DNA Stretching with Optical Tweezers

The experiment was repeated with the $Ru(phen)_3^{2+}$ complex. The single DNA molecule stretching curves in the presence of $Ru(phen)_3^{2+}$ are very similar to those for $Ru(phen)_2dppz^{2+}$ (Fig. 9a). An increase in both DNA length (a shift in the stretching curve to the right) and in the forces required to melt the DNA (an upward shift in the melting plateau) is seen with increasing concentrations of $Ru(phen)_3^{2+}$, which clearly illustrates that $Ru(phen)_3^{2+}$ intercalates. Importantly, in this case the concentrations of $Ru(phen)_3^{2+}$ required for intercalation occur in the micromolar range and saturation occurs around 750−1000 μM. These values suggest that $Ru(phen)_3^{2+}$ is a weaker intercalator than $Ru(phen)_2dppz^{2+}$, with approximately 3 orders of magnitude lower binding affinity. This fact is shown quantitatively by the value for $K_b = (8.8 \pm 0.3) \times 10^{3\ M-1}$ given by the fitting of the $Ru(phen)_3^{2+}$ binding curve obtained at 20 pN force (Fig. 9b). Interestingly, the binding site size for $Ru(phen)_3^{2+}$, $n = 3 \pm 0.2$, is similar to the same parameter obtained by this method for $Ru(phen)_2dppz^{2+}$, which is reasonable considering that the two complexes have the same charge and ancillary ligands. Again, the goodness of the fit of the data to the Mc Ghee-von Hippel model can be seen qualitatively from the overlap of the curve with almost all of the error bars, and quantitatively from the reduced χ^2 for the fit of 1.6. The $Ru(phen)_3^{2+}$ binding curve obtained at other low forces (5pN, 10pN) generates similar values for K_b and n (data not shown).

In contrast to the similarities between $Ru(phen)_2dppz^{2+}$ and $Ru(phen)_3^{2+}$, $Ru(bpy)_3^{2+}$ exhibits a strikingly different behavior for concentrations in the nanomolar and micromolar range. Little change is observed in the shape of the stretching curve with increasing $Ru(bpy)_3^{2+}$ (Fig. 9c).

In fact, the DNA stretching curves in the presence of $Ru(bpy)_3^{2+}$ resemble the stretching curves for naked dsDNA, indicating that this complex does not intercalate, at least not in this concentration regime. A very small and progressive increase in melting force is seen with the increase in ruthenium concentration, suggesting a minor stabilization of the DNA duplex due to external drug binding to DNA electrostatically or in the grooves. However, we cannot rule out the intercalation of the $Ru(bpy)_3^{2+}$ complex for all circumstances. At elevated ruthenium concentrations and at high stretching forces that would destabilize the DNA, it is likely that some intercalation of $Ru(bpy)_3^{2+}$ could occur. A small amount of lengthening seems to be present on the stretching curve of the dsDNA- $Ru(bpy)_3^{2+}$ complex at 100 μM drug concentration, but only at forces higher than 40 pN. Further experiments need to be performed in order to elucidate the characteristics of this "high force" binding mode for $Ru(bpy)_3^{2+}$.

Discussion

Intercalation of Ru(II) polypyridyl complexes examined by AFM

$Ru(bpy)_2dppz^{2+}$ is well established to be an intercalator, allowing us to focus on the benefits and limitations of the technique. With increasing amounts of metal complex between 1 and 12 μM, the average DNA molecules grow progressively longer as measured by AFM, clearly demonstrating that this molecule intercalates. This lengthening can be fit to a simple equilibrium expression to describe K_b and n. Interestingly, the value of K_b determined this way for $Ru(bpy)_2dppz^{2+}$ is approximately 10 to 100 times smaller than most published values for $Ru(bpy)_2dppz^{2+}$ and the values we determined using optical tweezers.[8,13] The "missing" binding affinity can be ascribed entirely to the presence of 5 mM Mg^{2+} in the AFM samples, because the binding of these complexes has a large electrostatic component.[8] Taking into account the divalent magnesium cations, the K_b determined by AFM agrees well with values determined using more traditional techniques. $Ru(bpy)_2dppx^{2+}$ is structurally similar to $Ru(bpy)_2dppz^{2+}$, differing only by two methyl groups. In the AFM experiments, the dppx complex behaves like its dppz parent: the two binding titration curves are nearly identical, and experiments with both complexes have the same limitations on high metal concentration. Literature values for the $Ru(bpy)_2dppx^{2+}$ equilibrium binding constant are on the order of 10^6 to 10^7 M^{-1} in dilute salt solution [13], similar to $Ru(bpy)_2dppz^{2+}$, so a K_b of 1.5×10^5 M^{-1} is reasonable under these solution conditions.

Because of the presence of Mg^{2+} ions, the binding constants for intercalation determined by AFM for polycationic molecules should be significantly diminished relative to solution studies as a general rule. As a result, the binding will be particularly difficult to measure for polycationic molecules with a small binding constant. Unfortunately, the presence of a multivalent cation like Mg^{2+} is required for the DNA to adhere to the negatively-charged mica surface. No atomically flat, positively-charged surfaces are currently available for AFM, and coating the mica with different polycations would be expected to have the same adverse effect on binding by Ru(II) complexes.

Even for the avid intercalator $Ru(bpy)_2dppz^{2+}$, in order to measure any DNA lengthening by AFM it is necessary to work at a very high Ru:bp ratio. To improve the fit of K_b and n, we should include higher ruthenium concentrations, but at 25μM ruthenium and above, the DNA no longer looks long nor straight, but is curly and clumped. It is likely that tertiary electrostatic interactions between the surface, the ruthenium complex, and the DNA dominate the behavior of the DNA and cause this change in shape. These kinds of interactions are not surprising, given the substantial literature about DNA condensation on mica.[43] A wide variety of polycations, including Mg^{2+}, Ni^{2+}, spermine, spermidine, and notably $Ru(NH_3)_6^{2+}$, cause DNA to form beautiful, complex shapes on mica such as toroids, rods, and "flowers".[44-49] It is thought that this polycation-induced condensation resembles the DNA condensation that is both common and necessary inside of cells and viruses. Our dilute DNA concentration prevents

the DNA from forming multi-stranded aggregates on the mica, but it is not unlikely that the DNA is looping around to align with itself in a condensation-like process mediated by the divalent ruthenium molecules. This condensation process also reflects the fact that at our higher concentrations, the concentration of ruthenium complexes vastly exceeds the concentration of base pairs. The binding of all of five Ru(II) complexes has a significant electrostatic contribution, so at very high Ru:bp ratios the excess ruthenium is almost certainly associated with the DNA extensively and non-intercalatively. This ruthenium-coated DNA could then spontaneously self-assemble on the mica surface.

In the cases of both $Ru(bpy)_2dppz^{2+}$ and $Ru(bpy)_2dppx^{2+}$ this AFM method predicts a neighbor exclusion number $n \cong 2$. This value is smaller than would be expected; a neighbor exclusion number around 2 is more common for a flat intercalator like ethidium bromide, but for Ru(II) polypyridyl complexes with their larger charge and bulky ancillary ligands, a larger binding site size on the order of 3 or more is reasonable.[7,8,50,51] $Ru(phen)_2dppz^{2+}$ molecules *will* bind to the DNA more frequently than once every three base pairs, but it is believed they do so nonintercalatively.[8] In our AFM method, only $Ru(bpy)_2dppz^{2+}$ molecules that cause lengthening (i.e. those that are intercalated) are counted, so any non-intercalating Ru(II) molecules should not affect n (though they may affect K_b). The AFM method may indicate that there are more molecules intercalated into the DNA at saturation than there "should" be due to experimental limitation: n cannot be determined from the occupancy at saturation since we cannot measure lengths at saturating Ru(II) concentrations. A second possibility is that tertiary binding to the Mg^{2+}-coated surface neutralizes charge repulsion between Ru(II) molecules and allows for a higher n than in solution.

There are insurmountable drawbacks to the AFM method for determining intercalation by the other Ru(II) polypyridyl complexes that bind DNA more weakly. Evidence from biophysical and spectroscopic studies would lead us to expect that $Ru(bpy)_2dpq^{2+}$ should intercalate, though ~100 times more weakly than $Ru(bpy)_2dppz^{2+}$ (*10*, *13*, *18*, *19*), that $Ru(phen)_3^{2+}$ might intercalate more weakly yet,[3,5-7,17] and that $Ru(bpy)_3^{2+}$ should not intercalate.[3] All this method allows us to conclude is that for the ruthenium polypyridyl complexes that intercalate into DNA more weakly than the dppz complexes, intercalation cannot be assessed within the proscribed concentration range, and thus cannot be measured. Our conclusion that AFM cannot measure intercalation of $Ru(phen)_3^{2+}$ and other weakly-binding Ru(II) complexes is distinctly different from that of Coury and coworkers, who examined the $Ru(phen)_3^{2+}$ complex by AFM and strongly asserted that it did not intercalate.[52] On careful comparison, it is clear that the data shown in that paper are consistent with ours (no lengthening observed at 1, 5 and 25 μM $Ru(phen)_3^{2+}$), but the conclusions are distinctly different. By placing $Ru(phen)_3^{2+}$ in the context of the ruthenium polypyridyl family, we demonstrate here that the absence of lengthening is an experimental limitation and not evidence against intercalation. As the earlier paper includes no images of ruthenium-bound DNA nor histograms of length distributions, it is not clear if the investigators faced the same issues of condensation, but notably their bar graphs show some modest *shortening* at 25 μM $Ru(phen)_3^{2+}$.

One important issue to discuss is that we have used racemic mixtures of the ruthenium complexes. It is known that the right- and left-handed complexes can have different binding constants and behaviors, though the differences between enantiomers are much smaller than the differences between different members of the Ru(II) polypyridyl complex family. Nonetheless, we are measuring binding of a mixture of two similar but nonidentical molecules in solution, and thus order-of-magnitude determinations of K_b and n reflect appropriate uncertainties. Our primary goal here was to broadly evaluate intercalation and to assess the value of single molecule methods using a variety of complexes. In order to get more accurate numbers it may be of interest to repeat some of the experiments with enantiopure Δ and Λ samples in the future. Notably, the presence of a racemic mixture cannot explain the

experimental difficulties AFM, because Coury and colleagues showed that the individual enantiomers of $Ru(phen)_3^{2+}$ behaved identically.[52]

Intercalation of Ru(II) complexes examined using DNA pulling with optical tweezers

DNA stretching using optical tweezers appears to be a much better method than AFM for studying intercalation of ruthenium(II) polypyridyl complexes into DNA, since the technique allows us to study complexes with different binding behaviors at a range of concentrations without serious condensation concerns. Our DNA stretching experiments directly demonstrate both stabilization of double-stranded DNA and lengthening of the DNA in the presence of $Ru(phen)_2dppz^{2+}$. These two properties are clearly consistent with a model in which $Ru(phen)_2dppz^{2+}$ intercalates and are inconsistent with other modes of binding. In addition, fits to a standard equilibrium binding model agree well with binding constant and binding site size estimates determined in bulk experiments.[8]

These data illustrate that DNA stretching experiments can reliably be used to detect intercalation events and determine intercalation parameters. Interestingly, the DNA stretching method clearly demonstrates DNA intercalation by $Ru(phen)_3^{2+}$. An increase in both contour length and the force required to pull the DNA strands apart is apart is interpreted by categorizing $Ru(phen)_3^{2+}$ as an intercalator. This behavior is inconsistent with electrostatic or groove binding alone, although these binding modes may also occur and are not detected by this method.

Furthermore, these stretching curves allow us to make quantitative measurements of the Ru (II) binding affinity to DNA and thus demonstrate that $Ru(phen)_3^{2+}$ binds roughly three orders of magnitude more weakly than $Ru(phen)_2dppz^{2+}$. This intercalative binding constant is merely an approximation, since the Mc Ghee- von Hippel model describes a classical intercalator like ethidium. $Ru(phen)_3^{2+}$ would be expected to have a much more complicated interaction with DNA, especially as a racemic mixture and at high concentrations. However, it is important to note that the data fit well to the Mc Ghee- von Hippel intercalation model, as seen by the shape of the curve, the overlap with the error bars, and the reduced χ^2 value for the fit (Fig. 8b). Thus, despite the complexity of the system, we propose that fits of the DNA stretching data to a classical intercalation model provide a sound *estimate* of the intercalative binding constant. This estimate provides a useful indication of how weak the intercalation of $Ru(phen)_3^{2+}$ is, and how rare an intercalation event would be at normal low ruthenium concentrations.

Our demonstration of intercalation by $Ru(phen)_3^{2+}$ is clearly provocative, given that electrostatic or groove-binding and partial intercalation are currently favored by most groups as the major modes of binding. However, the DNA stretching method selectively detects intercalation events, which may represent a small fraction of the molecules in the solution under most conditions given the millimolar binding constant. Moreover optical tweezers experiments are performed at a very high Ru:DNA ratio. This high loading may favor an intercalative mode over an electrostatic or groove-binding mode.[7] Alternatively, perhaps pulling the DNA out straight and not allowing it to kink or condense selectively promotes intercalation over groove and electrostatic binding. (Note that we observe intercalation at very low forces, so the pulling itself should not open the base pairs enough to cause intercalation). Regardless of the cause, the data are clearly most consistent with intercalation by $Ru(phen)_3^{2+}$ in this experimental system. These results agree with much of the previously published literature, despite the apparent controversies in interpretation about the binding of $Ru(phen)_3^{2+}$. For example, the length changes revealed by the optical tweezers are not inconsistent with viscometric studies of DNA length changes that revealed modest DNA lengthening, but only at high racemic $Ru(phen)_3^{2+}$ concentrations.[6,51] The increase in duplex stability is also consistent with UV melting temperature experiments that demonstrated an increase in DNA stability in the presence of both isomers of $Ru(phen)_3^{2+}$.[51]

The experimental data also reveal new details about the interaction between single DNA molecules and $Ru(bpy)_3^{2+}$. The complex is well known not to intercalate in bulk solution, but we see some hints here that at very high concentrations *and* high forces, it may intercalate into DNA. This leads us to consider whether intercalation into DNA may need to be examined in more detail under naturally occurring situations where the DNA may be destabilized and stretched out into non-B-form conformations.

These experiments also raise a series of other questions and ideas for new experiments using DNA pulling with optical tweezers. Clearly, the mechanism of binding at high forces is a new area of exploration, but it would also be interesting to pursue sequence preference using other DNA sequences, the binding of other members of the ruthenium(II) polypyridyl family, as well as the differences between the enantiomers of individual complexes. We plan to explore the role of charge in intercalation using other related organometallic complexes. The progressive changes in the shapes of the stretching curves and the mechanism of possible cooperativity in the melting transition also will be active areas of further exploration.

Examining small-molecule binding to DNA using single-molecule techniques

Single molecule techniques have some clear benefits for examining intercalation into DNA. These data demonstrate that AFM is not a good method for examining Ru(II) polypyridyl complexes but do not preclude using AFM to examine binding by other putative intercalators with reasonably large K_b's and +1 or no charge in solution as shown previously.[21-25] These molecules have low affinity for the surface of the mica and for the DNA backbone, and thus do not cause condensation. In terms of information content, established spectroscopic methods (CD, LD, NMR, UV-vis, fluorescence) can provide more detailed information about intercalator-DNA interactions, including major vs. minor groove preference, partial vs. full intercalation, and sequence preferences. Because of the relatively simple nature of the AFM intercalation experiments, less information can be garnered from them, but DNA lengthening by AFM has the major advantage that it is easy to measure and interpret. Overall, with attention to the particular chemical system and surface, AFM can be employed productively for studying small-molecule binding.

The DNA force-induced melting technique using an optical tweezers instrument has some important advantages compared to AFM and bulk methods. In the present study, we obtain direct molecular length measurements as a function of intercalating ligand concentration, resulting in equilibrium binding titrations with high accuracy and reproducibility. These experiments can be performed under conditions that preclude other types of measurements, such as conditions that induce DNA condensation or aggregation. As shown here with $Ru(phen)_3^{2+}$, this method for quantifying ligand binding is most sensitive to intercalative binding, so other binding modes such as electrostatic or minor groove binding do not significantly contribute to our results. In contrast, optical measurements are sometimes complicated by the necessity of distinguishing between various binding modes that contribute to the observed signal. We have previously demonstrated that this method can be useful for studying other types of intercalators, including molecules that are charged or neutral, and stronger or weaker binders.[30] In addition, due to the fact that it requires very little material, this technique has a potential use in drug screening assays. The DNA force-induced melting technique focuses on individual molecules and reveals fine details that could be lost due to ensemble averaging. In the absence of a binding ligand, this method has been used to characterize DNA elasticity and stability in unprecedented detail.[26] It can also be used to determine the effects of DNA binding ligands on equilibrium DNA melting free energy[53], ligand binding free energy[54], and binding kinetics[55,56].

Conclusions

Both atomic force microscopy and optical tweezers have been used here to examine intercalation into DNA by a family of ruthenium(II) polypyridyl complexes. Though atomic force microscopy has limited use for examining intercalation by divalent cations because of interference from surface-binding phenomena, DNA pulling with optical tweezers is an excellent method for examining ruthenium(II) binding to DNA. Results of DNA pulling experiments confirm previous results measured with other techniques in the bulk phase, specifically the absence of intercalation by $Ru(bpy)_3^{2+}$ as well as strong intercalation by $Ru(phen)_2dppz^{2+}$. Finally, we present clear evidence that $Ru(phen)_3^{2+}$, whose binding has been a matter of controversy for many years, does intercalate at high metal complex concentrations.

Supplementary Material

Refer to Web version on PubMed Central for supplementary material.

Acknowledgments

We would like to thank Dr. B. Lane for his assistance in data fitting, Dr. I. Rouzina for helpful discussions, and Professor E. D. A. Stemp and Dr. S. Delaney for metal complexes.

References

1. Kumar CV, Barton JK, Turro NJ. J. Am. Chem. Soc 1985;107:5518–5523.
2. Barton JK, Goldberg JM, Kumar CV, Turro NJ. J. Am. Chem. Soc 1986;108:2081–2088.
3. Pyle AM, Rehmann JP, Meshoyrer R, Kumar CV, Turro NJ, Barton JK. J. Am. Chem. Soc 1989;111:3051–3058.
4. Hiort C, Nordén B, Rodger A. J. Am. Chem. Soc 1990;112:1971–1982.
5. Lincoln P, Nordén B. J. Phys. Chem. B 1998;102:9583–9594.
6. Satyanarayana S, Dabrowaik JC, Chaires JB. Biochemistry 1992;31:9319–9324. [PubMed: 1390718]
7. Coggan DZM, Haworth IS, Bates PJ, Robinson A, Rodger A. Inorg. Chem 1999;38:4486–4497. [PubMed: 11671161]
8. Haq I, Lincoln P, Suh D, Nordén B, Chowdhry B, Chaires JB. J. Am. Chem. Soc 1995;117:4788–4796.
9. Friedman AE, Chambron J-C, Sauvage J-P, Turro NJ, Barton JK. J. Am. Chem. Soc 1990;112:4960–4962.
10. Collins JG, Sleeman AD, Aldrich-Wright JR, Greguric I, Hambley TW. Inorg. Chem 1998;37:3133–3141.
11. Jenkins Y, Friedman AE, Turro NJ, Barton JK. Biochemistry 1992;31:10809–10816. [PubMed: 1420195]
12. Stemp EDA, Arkin MR, Barton JK. J. Am. Chem. Soc 1997;119:2921–2925.
13. Delaney S, Pascaly M, Bhattacharya P, Han K, Barton JK. Inorg. Chem 2002;41:1966–1974. [PubMed: 11925195]
14. Dupureur CM, Barton JK. Inorg. Chem 1997;36:33–43.
15. Rehmann JP, Barton JK. Biochemistry 1990;29:1701–1709. [PubMed: 2331459]
16. Eriksson M, Leijon M, Hiort C, Nordén B, Gräslund A. Biochemistry 1994;33:5031–5040. [PubMed: 8172878]
17. Gisselfält K, Lincoln P, Nordén B, Jonsson M. J. Phys. Chem. B 2000;104:3651–3659.
18. Greguric I, Aldrich-Wright JR, Collins JG. J. Am. Chem. Soc 1997;119:3621–3622.
19. Collins JG, Aldrich-Wright JR, Greguric I, Pellegrini PA. Inorg. Chem 1999;38:5502–5509. [PubMed: 11671277]
20. Bloomfield, V.; Crothers, D.; Tinoco, I. Nucleic Acids: Structures, Properties, and Functions. University Science Books; Sausalito, California: 2000.

21. Coury J, McFail-Isom L, Dean Williams L, Bottomley LA. Proc. Natl. Acad. Sci. USA 1996;93:12283–12286. [PubMed: 8901572]
22. Bordelon JA, Feiera KJ, Siddiqui S, Wright LL, Petty JT. J. Phys. Chem 2002;B. 106:4838–4843.
23. Berge T, Jenkins NS, Hopkirk RB, Waring MJ, Edwardson JM, Henderson RM. Nuc. Acids Res 2002;30(13):2980–2986.
24. Berge T, Haken EL, Waring MJ, Henderson RM. J. Struct. Biol 2003;142:241–246. [PubMed: 12713951]
25. Tseng YD, Ge H, Wang X, Edwardson JM, Waring MJ, Fitzgerald WJ, Henderson RM. J. Mol. Biol 2005;345:745–758. [PubMed: 15588823]
26. Williams MC, Rouzina I, Bloomfield V. Acc. Chem. Res 2002;35:159–166. [PubMed: 11900519]
27. Williams MC, Rouzina I. Curr. Op. Struct. Biol 2002;12:330–336.
28. Baumann CG, Smith SB, Bloomfield V, Bustamante C. Proc. Natl. Acad. Sci 1997;94:6185–6190. [PubMed: 9177192]
29. Wenner JR, Williams MC, Rouzina I, Bloomfield V. Biophys. J 2002;82:3160–3169. [PubMed: 12023240]
30. Vladescu ID, McCauley MJ, Rouzina I, Williams MC. Phys. Rev. Lett 2005;95:158102. [PubMed: 16241765]
31. Krautbauer R, Pope LH, Schrader TE, Allen S, Gaub HE. FEBS Lett 2002;510:154–158. [PubMed: 11801245]
32. Krautbauer R, Fischerlander S, Allen S, Gaub HE. Single Molecules 2002;3:97–103.
33. Eckel R, Ros R, Ros A, Wilking SD, Sewald N, Anselmetti D. Biophys. J 2003;85:1968–1973. [PubMed: 12944309]
34. Tessmer I, Baumann CG, Skinner GM, Molloy JE, Hoggett JG, Tendler SJB, Allen S. J. Modern Optics 2003;50:1627–1636.
35. Sischka A, Toensing K, Eckel R, Wilking SD, Sewald N, Ros R, Anselmetti D. Biophys. J 2005;88:404–411. [PubMed: 15516529]
36. Amouyal E, Homsi A, Chambron J-C, Sauvage J-P. J. Chem. Soc., Dalton Trans 1990;6:1841–1845.
37. Flannery, BP.; Teukolsky, SA.; Vetterling, WT. Numerical Recipes in C. Cambridge University Press; Cambridge: 1988.
38. McCauley M, Hardwidge PR, Maher LJ, Williams MC. Biophys. J 2005;89:353–364. [PubMed: 15833996]
39. McGhee JD, von Hippel PH. J. Mol. Biol 1974;86:469–489. [PubMed: 4416620]
40. McGhee JD. Biopolymers 1976;15:1345–1375. [PubMed: 949539]
41. Hansma H. Annu. Rev. Phys. Chem 2001;52:71–92. [PubMed: 11326059]
42. Lyubchenko YL. Cell. Biochem. Biophys 2004;41:75–98. [PubMed: 15371641]
43. Bloomfield V. Curr. Op. Struct. Biol 1996;6:334–341.
44. Golan R, Pietrasanta L, Hsieh W, Hansma H. Biochemistry 1999;38:14069–14076. [PubMed: 10529254]
45. Ono MY, Spain EM. J. Am. Chem. Soc 1999;121:7330–7334.
46. Fang Y, Hoh J. Nuc. Acids Res 1998;26:588–593.
47. Martin AL, Davies MC, Rackstraw BJ, Roberts CJ, Stolnik S, Tendler SJB, Williams PM. FEBS Lett 2000;480:106–112. [PubMed: 11034309]
48. Dunlap DD, Maggi A, Soria MR, Monaco L. Nuc. Acids Res 1997;25:3095–3101.
49. Liu D, Wang C, Li J, Lin Z, Tan Z, Bai C. J. Biomol. Struct. Dyn 2000;18:1–9. [PubMed: 11021648]
50. Holmlin RE, Stemp EDA, Barton JK. Inorg. Chem 1998;37:29–34. [PubMed: 11670256]
51. Satyanarayana S, Dabrowaik JC, Chaires JB. Biochemistry 1993;32:2573–2584. [PubMed: 8448115]
52. Coury J, Anderson JR, McFail L, Dean Williams L, Bottomley LA. J. Am. Chem. Soc 1997;119:3792–3796.
53. Pant K, Karpel RL, Williams MC. J. Mol. Biol 2003;327:571–578. [PubMed: 12634053]
54. Pant K, Karpel RL, Rouzina I, Williams MC. J. Mol. Biol 2005;349:317–330. [PubMed: 15890198]
55. Pant K, Karpel RL, Rouzina I, Williams MC. J. Mol. Biol 2004;336:851–870. [PubMed: 15095865]

56. Sokolov IM, Metzler R, Pant K, Williams MC. Biophys. J 2005;89:895–902. [PubMed: 15908574]

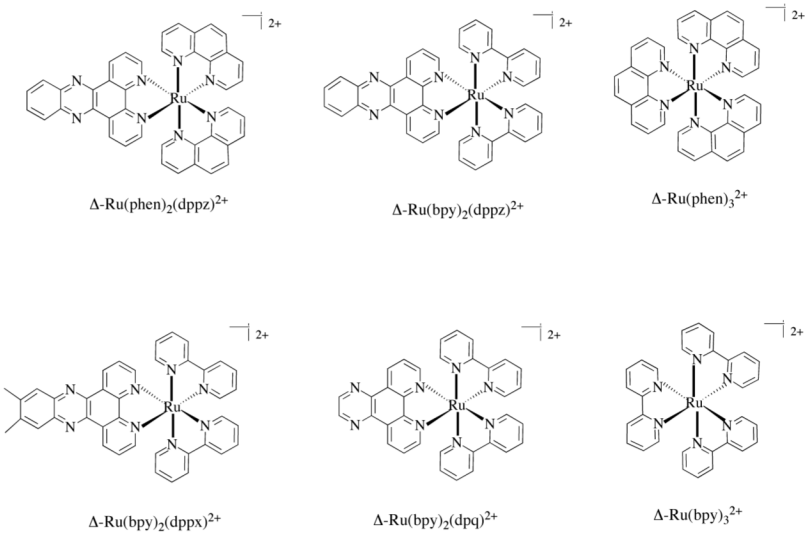

Figure 1. Structures of the ruthenium complexes used in this study

The shortened names under each structure will be used throughout this paper. Only the right-handed (Δ) enantiomers are shown here, though the racemic mixtures were used in these studies.

(a)

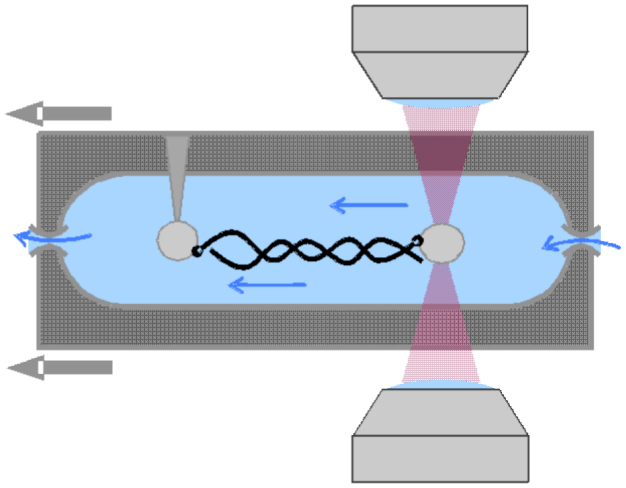

(b)

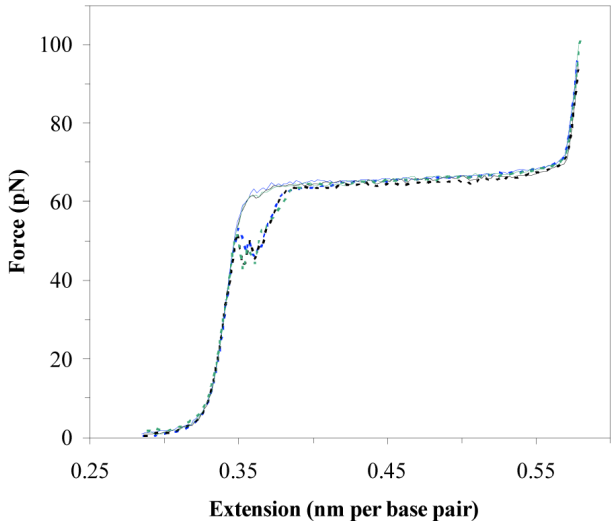

Figure 2. DNA stretching experiments

(a) Biotin labeled DNA (black) is extended between two streptavidin-coated beads (grey) held by a micropipette tip and an optical trap (red). Arrows indicate the direction that the solution flows through the flow cell. (b) Force extension (solid lines) and relaxation data (dotted lines) for DNA in 10 mM Hepes pH 7.5, 50 mM Na^+.

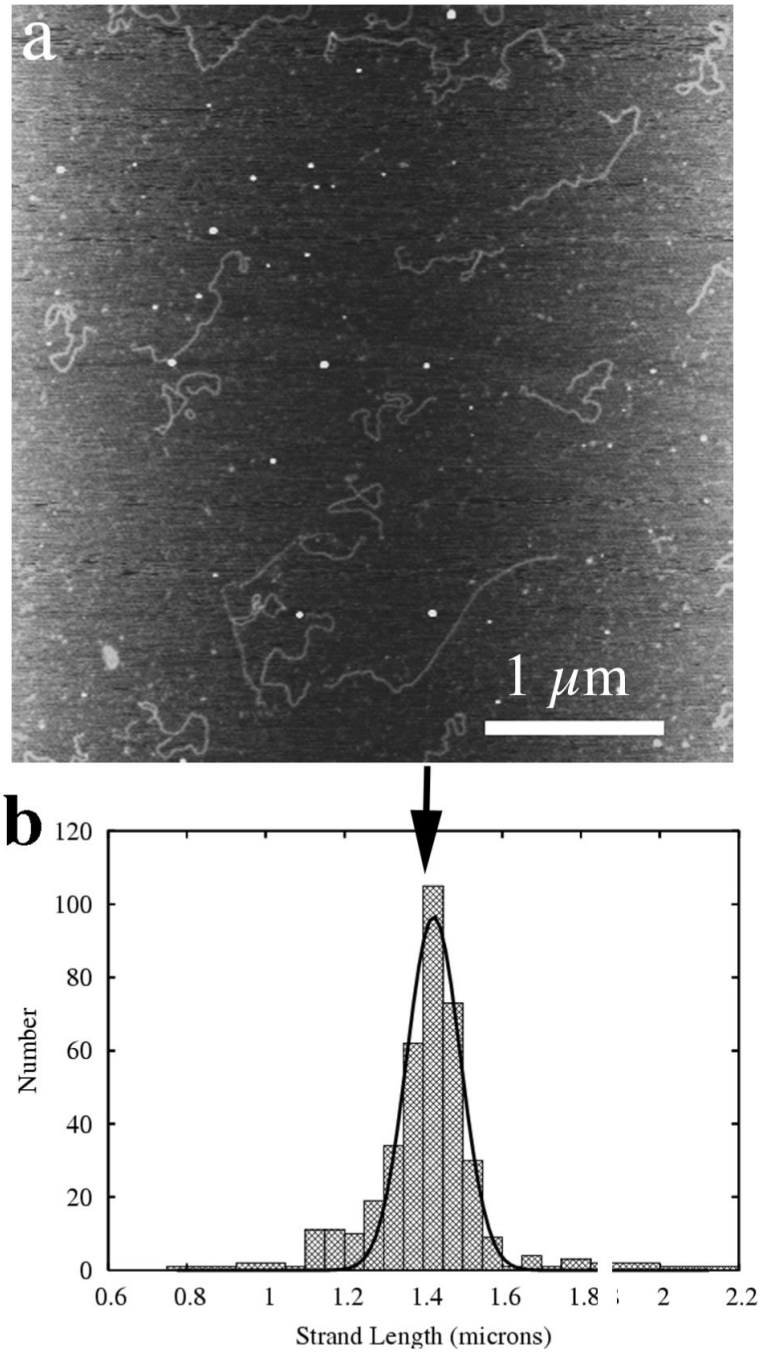

Figure 3. Determining the length of DNA by AFM

(a) An atomic force microscope image showing several pieces of DNA on a cleaved mica substrate. All are 1461-base-pair, double-stranded restriction fragments derived from pBR322. (b) Histogram of the measured lengths of individual DNA molecules. The mean measured length of the DNA molecules is 1.43 ± 0.03 μm (black arrow); the calculated length of the DNA is 1.46 μm, based on a 0.34 nm base pair step.

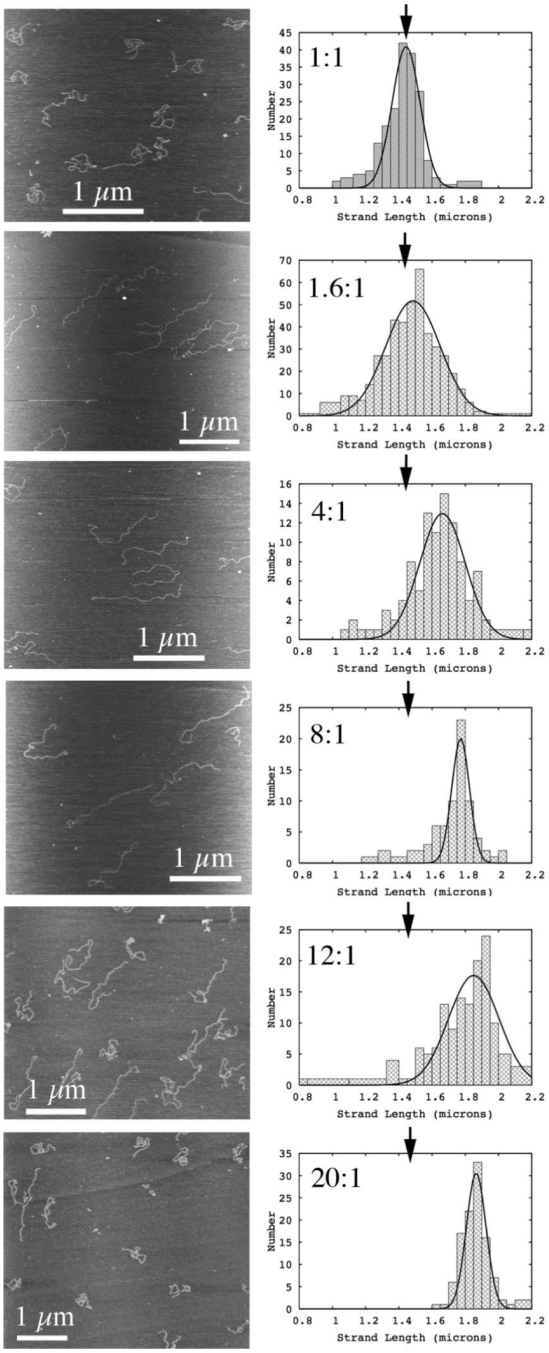

Figure 4. DNA lengthening due to intercalative binding by $Ru(bpy)_2dppz^{2+}$

Characteristic AFM images and histograms of DNA length are shown for six ruthenium concentrations: (a) 750 nM Ru, or 1:1 Ru:base pairs (b) 1.2 μM Ru, or 1.6:1 Ru:base pairs (c) 3 μM, or 4:1 Ru:base pairs (d) 6 μM, or 8:1 Ru:base pairs (e) 9.0 μM or 12:1 Ru:base pairs (f) 15 μM, or 20:1 Ru:base pairs. The DNA concentration is 750 nM base pairs in all cases. The mean measured length of the DNA molecules alone is 1.43 ± 0.03 μm (black arrows).

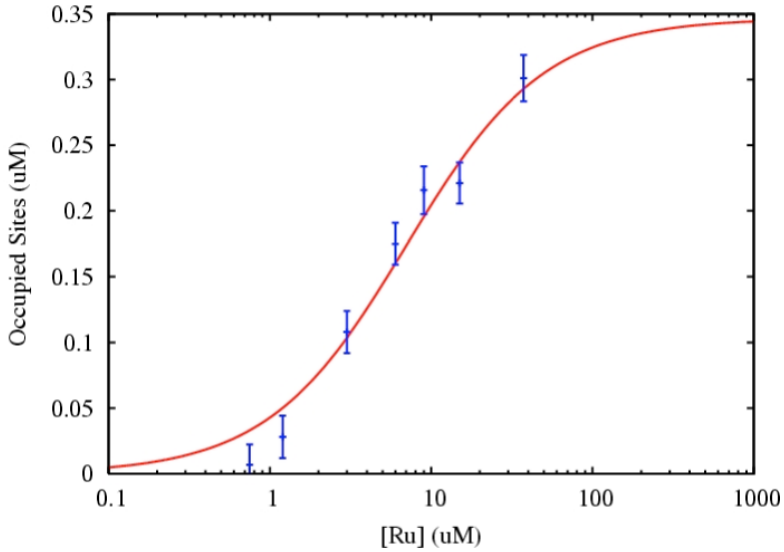

Figure 5. Calculating K_b and n for intercalation by $Ru(bpy)_2dppz^{2+}$

(a) Concentration of occupied intercalation sites as a function of ruthenium concentration. Line represents best fit to the data, $K_b = 1.5 \pm 0.7 \times 10^5\ M^{-1}$, n = 2.1 ± 0.4.

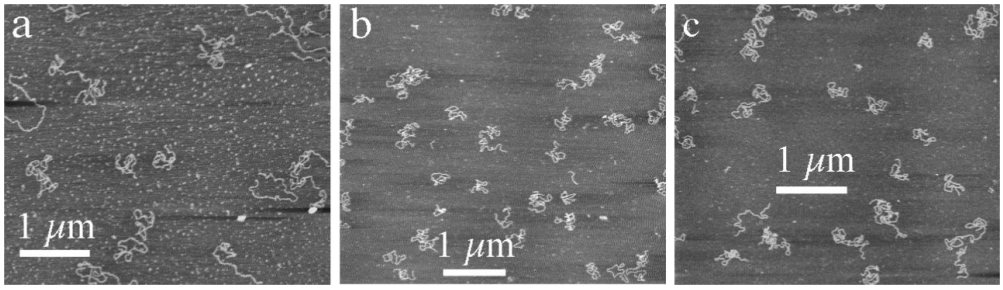

Figure 6. AFM images with high concentrations of ruthenium(II) complex

(a) 50:1 $Ru(bpy)_2(dppz)^{2+}$ to base pairs, or 37 μM (b) 50:1 $Ru(phen)_3^{2+}$, or 37 μM (c) 50:1 $Ru(bpy)_3^{2+}$, or 37 μM. Note that the DNA is generally curled up, which makes it difficult or impossible to measure most or all of the molecules. Those that can be measured sometimes appear *shorter* than DNA with less bound Ru(II). Also, the mica surface can be hydrophobic and the tip does not track across the surface well.

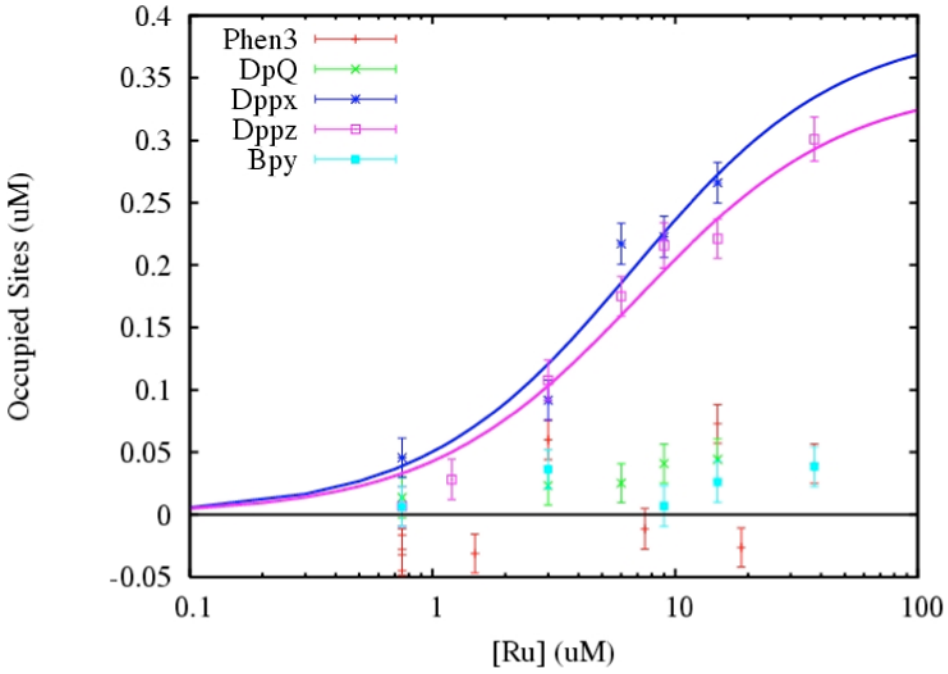

Figure 7. DNA Binding curves for five ruthenium octahedral complexes, as determined by AFM

The concentration of occupied base pairs is shown as a function of Ru(II) concentration for the five complexes studied here: $Ru(bpy)_2dppz^{2+}$, $Ru(phen)_3^{2+}$, $Ru(bpy)_3^{2+}$, $Ru(bpy)_2dppx^{2+}$, $Ru(bpy)_2dpq^{2+}$. Curves represent fits to the values shown in Table 1.

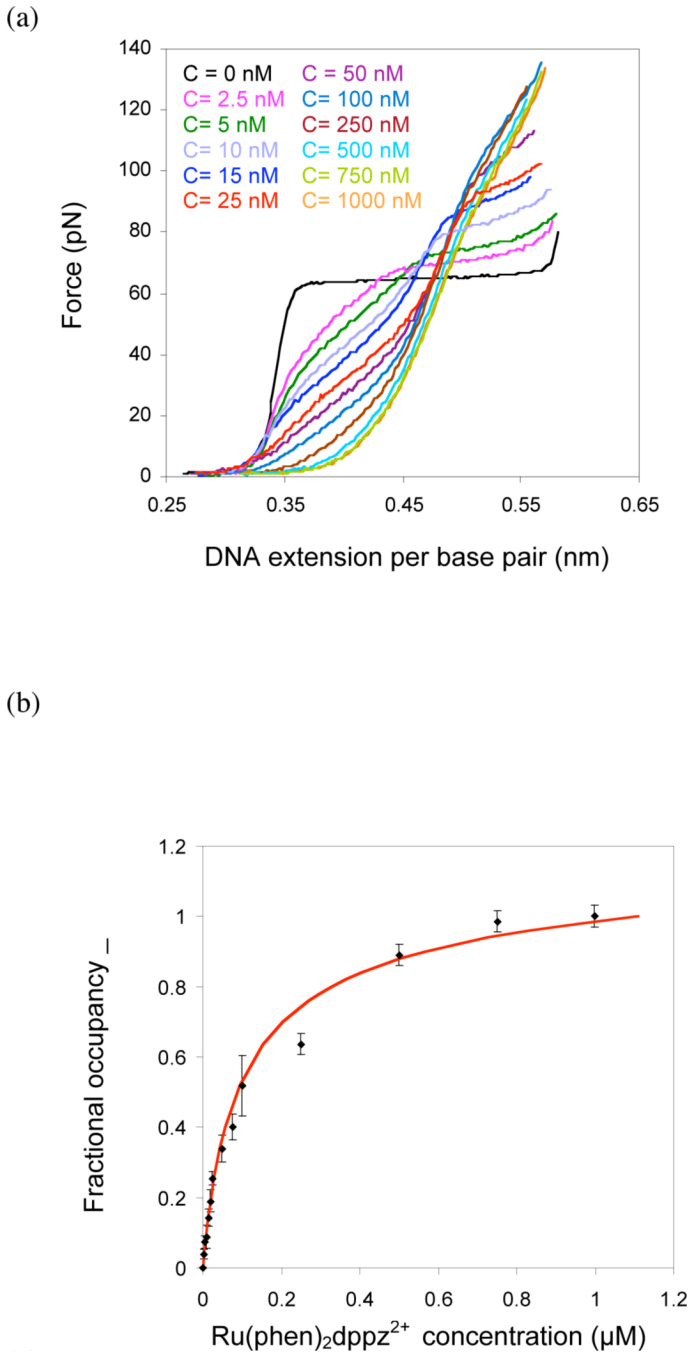

Figure 8. DNA pulling using optical tweezers in the presence of $Ru(phen)_2dppz^{2+}$

(a) DNA extension vs. force curves are shown for a range of concentrations of $Ru(phen)_2dppz^{2+}$. The black line is the force-extension curve for DNA alone. The $Ru(phen)_2dppz^{2+}$ reaches saturation around 750 nm. (b) A Binding titration curve is determined from the extension vs. force data. The fractional occupancy Θ is shown as a function of ruthenium concentration at 10 pN of force. The binding curve represents the best fit to the McGhee-von Hippel model (Eqn. 7) and the binding constant and neighbor exclusion number shown in Table 1.

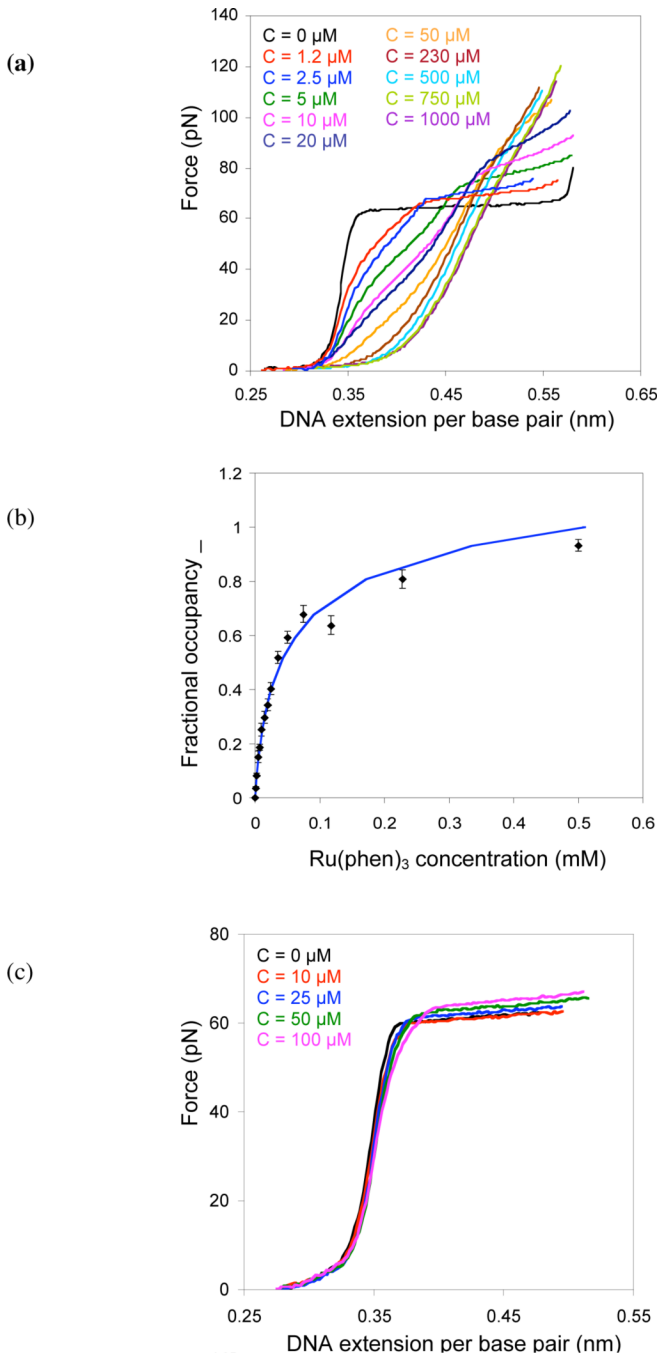

Figure 9. DNA pulling using optical tweezers in the presence of $Ru(phen)_3^{2+}$ or $Ru(bpy)_3^{2+}$

(a) DNA extension vs. force curves are shown for a range of concentrations of $Ru(phen)_3^{2+}$. The black line is the force-extension curve for DNA alone. The $Ru(phen)_3^{2+}$ reaches saturation around 750 μm. (b) The fractional occupancy Θ is shown as a function of $Ru(phen)_3^{2+}$ concentration at 20 pN of force. The binding curve represents the best fit to equation 7 and the binding constant and neighbor exclusion number shown in Table 1. (c) DNA extension vs. force curves are shown for a range of concentrations of $Ru(bpy)_3^{2+}$.

Table 1

Complex	*Number of rings in largest ligand*	*dsDNA binding constant* (K_b) *and binding site size* (n)	
		AFM[a]	*DNA stretching*[b]
$Ru(bpy)_2$**dppz**$^{2+}$ or $Ru(phen)_2$**dppz**$^{2+}$	5	$K_b = (1.5 \pm 0.7) \times 10^5\ M^{-1}$ n = 2.2 ± 0.4	$K_b = (3.2 \pm 0.1) \times 10^6\ M^{-1}$ n = 3 ± 0.5
$Ru(bpy)_2$**dppx**$^{2+}$	5	$K_b = (1.5 \pm 0.7) \times 10^5\ M^{-1}$ n = 1.9 ± 0.4	------
$Ru(bpy)_2$ **dpq**$^{2+}$	4	Cannot be determined but $K_b \leq 10^4\ M^{-1}$	------
Ru(**phen**)$_3^{2+}$	3	Cannot be determined but $K_b \leq 10^4\ M^{-1}$	$K_b = (8.8 \pm 0.3) \times 10^3\ M^{-1}$ n = 3 ± 0.2
Ru(**bpy**)$_3^{2+}$	2	Cannot be determined but $K_b \leq 10^4\ M^{-1}$	No intercalation observed

[a] performed in 10 mM Tris pH 7.5, 1 mM EDTA, 5 mM $MgCl_2$

[b] performed in 10 mM Hepes pH 7.5, 95 mM NaCl, 5 mM NaOH